

Exchange splitting and critical-point binding energies for iron (110)

A. M. Turner and J. L. Erskine

Department of Physics, University of Texas, Austin, Texas 78712

(Received 21 August 1981)

The exchange splitting and several critical-point binding energies along Γ - Σ - N of the Brillouin zone for ferromagnetic iron have been determined using angle-resolved photoemission. The room-temperature exchange splitting at Γ is determined to be 2.08 eV, and critical-point energies obtained from experimental data are found to be in good agreement with theoretical predictions.

The bulk and surface electronic properties of transition metals have been a subject of appreciable interest in recent years. Work in this area has focused primarily on the electronic properties of nickel, however, corresponding experimental and theoretical results for iron are now beginning to appear. Many of the issues which have tended to draw interest to the intrinsic electronic and magnetic properties of nickel are now understood although several important questions reflecting different viewpoints apparently remain to be settled.¹⁻³ Additional insight into these unsettled issues could be derived from studies of related metals, in particular iron.

The literature covering bulk and surface electronic structure of iron is not nearly as extensive as that for nickel. Bulk⁴ and surface⁵⁻⁸ electronic structure calculations have been carried out and several angle-resolved photoemission studies of the high symmetry iron crystal faces have been reported.⁹⁻¹² Heimann and Neddermeyer⁹ concluded that most of the features observed in their angle-resolved energy-distribution curves (AREDC's) resulted from surface photoemission and density of states effects. Schultz *et al.*¹⁰ reached a similar conclusion in discussing their data. Kevan *et al.*¹¹ found that their data for Fe(100) supported results for $E(k)$ along the (010) azimuth obtained from an interpolation scheme applied to Callaway and Wang's⁴ band calculation. Eastman *et al.*¹² also found good agreement with calculated bands along Γ - P - N by applying a direct transition model based on a free electron final band to AREDC's obtained from an Fe(111) crystal face.

In this Report, we report angle-resolved photoemission results for an Fe(110) surface which show that a direct transition model based on a free electron final band accounts for all significant structures in the measured normal emission AREDC's in terms of the band structure obtained by Callaway and Wang.⁴ We obtain the exchange splitting at Γ and a number of critical point binding energies along Γ - Σ - N in the bulk Brillouin zone.

Experiments reported here were conducted using

an Auger-photoelectron spectrometer which has been described previously.¹³ Photoelectrons were produced by radiation from a high intensity resonance lamp. By using different gases and operating pressures, we have found that rare gas resonance lines provide a good selection of photon energies ranging from 8.44 to 48.38 eV.

The iron single crystals were spark cut and aligned to approximately $\pm 1^\circ$ using x-ray Laue techniques and mechanically polished to a mirror surface using alumina powder to 0.05 μm size. To reduce bulk impurities, mainly sulphur, the crystals were heated at $\approx 800^\circ\text{C}$ for several weeks in a flowing hydrogen atmosphere (10 mol% H_2 90 mol% Ar). Subsequent *in situ* cleaning involved standard cycles of argon ion sputtering (500 eV) and annealing at 500–850 $^\circ\text{C}$. Clean surfaces exhibited an oxygen Auger peak (530 eV) about 1/10 the intensity of the Fe peak at 562 eV. This ratio corresponds to an oxygen coverage of a few percent of a monolayer. Other impurity Auger lines were considerably weaker. Our cleaning procedure also produced excellent low-energy electron diffraction (LEED) patterns.

Symmetry selection rules associated with electric dipole transitions and conservation laws associated with the photoemission process provide a basis for direct interpretation of AREDC's.¹⁴ In the direct-transition model of photoemission, components of momentum parallel to the crystal surface k_{11} are conserved, and the electron energies are related by

$$E_f = E_i + \hbar\omega, \quad E = E_f + V_0,$$

where E_f and E_i are the final and initial states in the crystal, E is the kinetic energy of the photoemitted electron in vacuum, and $\hbar\omega$ is the photon energy. V_0 is the crystal inner potential. Since k_{11} is conserved it can be determined directly from the exit angle and E . The perpendicular component of the momentum k_{\perp} can be determined if the dispersion of the final state band is known. In many cases, a free-electron final band has worked very well¹⁵ although the actual

dispersion of the final band can be determined directly, in principle.^{14,15} In the work reported here, we are able to place the final band based on our experimental data. The final band dispersion is given by

$$k_{\perp} = \frac{1}{\hbar} [2m(E + V_0) - \hbar^2 k_{\parallel}^2]^{1/2},$$

where, in normal emission, $k_{\parallel} = 0$.

Figure 1 shows normal emission AREDC's for Fe(110) with $\Delta\Omega = 4^\circ$ and energy resolution of ~ 100 meV. Peaks (and shoulders) are identified by letters and the inset table shows the binding energy measured from the Fermi energy E_F for each peak. These peaks correspond to initial states along the Γ - Σ - N direction in the bulk Brillouin zone, and possibly to surface states at Γ in the surface Brillouin zone for the (110) face.

Figure 2 shows the calculated bands of ferromagnetic iron along Γ - Σ - N of the bulk Brillouin zone.⁴ Of the bands shown, only initial state bands having Σ_1 , Σ_3 , or Σ_4 symmetry can be detected in normal emission geometry.^{16,17} Polarized light can be used to distinguish between the allowed initial state symmetries. In our experiments, unpolarized light incident at about 30° from the sample normal was used. Refraction effects can account for some polari-

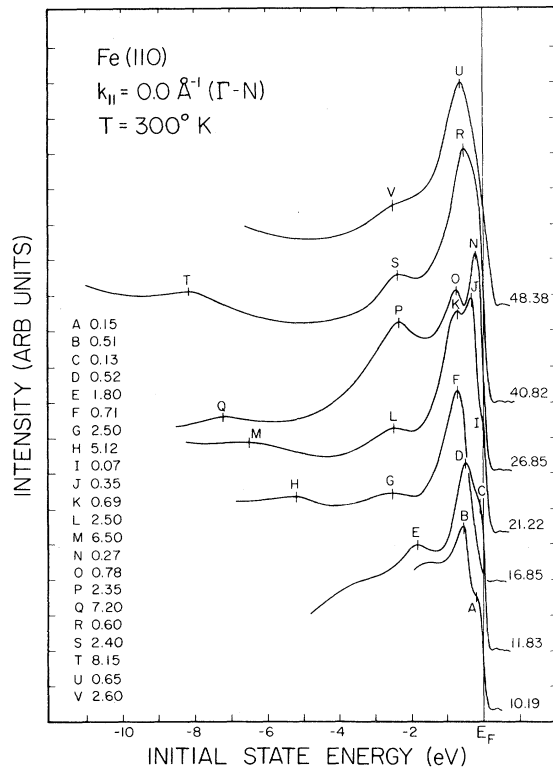


FIG. 1. Normal emission AREDC's for a Fe(110) surface at room temperature.

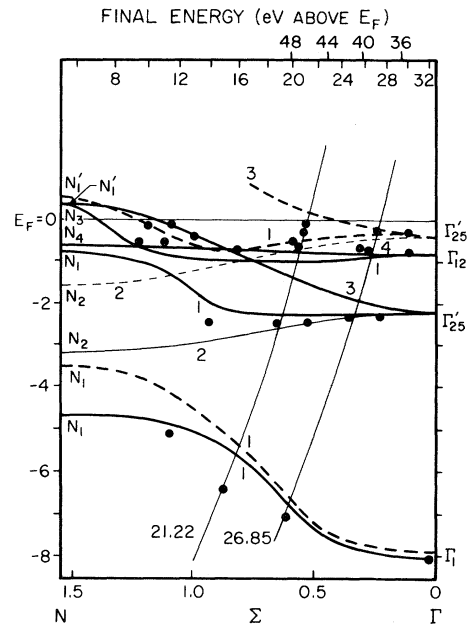


FIG. 2. Calculated energy bands for ferromagnetic iron (Ref. 4) along Γ - Σ - N . Heavy solid lines represent majority spin bands. Heavy dashed lines represent minority spin bands. Σ_2 bands (dipole forbidden in normal emission) are represented by light lines. The final (free electron) band energy is plotted along the top of the figure.

zation effects, however, for the present discussion we only wish to point out that our experimental conditions permit all allowed transitions to be excited. No evidence for Σ_2 (forbidden) bands were observed. Several features, in particular, those marked N and J , appear more sensitive to fractional monolayer coverages of oxygen or sulphur than other bulk features. This behavior suggests that surface states might be contributing some emission intensity to these features which we later show correspond to bulk states.

The free electron final band was determined by following the lower sp band dispersion to the Γ_1 point. In this particular case, the resonance lines available from various gas discharges (8.44 to 48.38 eV) permit tracking the sp band sufficiently close to Γ_1 , to determine the final band. Once the final band is determined, the binding energies of all the peaks can be mapped onto the appropriate point along the Γ - Σ - N direction. These points are shown on Fig. 2, and the resulting critical point energies are tabulated in Table I. The uncertainties indicated in Table I reflect the accuracy of our determination of the final band and of the various peak centers by a curve-fitting technique outlined below.

The room-temperature exchange splitting at Γ ($\delta E_{ex} = \Gamma_{251} - \Gamma_{251}$) is 2.08 eV. This value is some-

TABLE I. Experimental and theoretical binding energies along Γ - Σ - N for ferromagnetic iron. Theoretical bands are from Ref. 4.

Symmetry point	Binding energy (eV)	
	This experiment	Callaway and Wang
$\Gamma_{25\downarrow}$	0.27 ± 0.05	0.40
$\Gamma_{12\uparrow}$	0.78 ± 0.05	0.86
$\Gamma_{25\uparrow}$	2.35 ± 0.10	2.18
Γ_1	8.15 ± 0.10	8.11
$\Sigma_{1\uparrow}$ lower	2.10 ± 0.20	2.32
$\Sigma_{1\downarrow}$	5.90 ± 0.25	5.83

what larger than the value at P ,¹² therefore, it is clear that majority and minority spin bands have different dispersion as found previously.¹¹ An attempt was made to measure the temperature dependence of δE_{ex} near Σ by heating the sample.¹⁸ Figure 3 shows two AREDC's taken at $\hbar\omega = 21.22$ eV, one at room temperature and one at 710 °C. Perturbations resulting from heating pulses were avoided by gating off the counting system while current was applied to the sample.

A curve fitting routine based on Gaussian functions was used to decompose our AREDC's.¹⁹ The primary motivation for this procedure was to obtain accurate values for peak locations and estimates of their widths and relative strengths. Decompositions of the two spectra in Fig. 3 are shown based on seven Gaussians for the clean room-temperature data and eight Gaussians for the 710 °C data. The extra Gaussian for the heated sample accounts for a small amount of sulphur (~ 0.1 monolayer) which diffuses to the surface during heating above 600 °C. Five peaks are clearly seen in the room-temperature AREDC's and these are assigned to the five allowed transitions ($\Sigma_{1\downarrow}$, $\Sigma_{1\uparrow}$, $\Sigma_{4\uparrow}$, $\Sigma_{1\downarrow}$, and $\Sigma_{3\downarrow}$). The lower $\Sigma_{1\uparrow}$ band is needed to obtain the correct shape of the large peak resulting primarily from the $\Sigma_{4\uparrow}$ band. High resolution is required to observe the $\Sigma_{3\downarrow}$ band which is very near E_F . The large difference in strength of the $\Sigma_{1\uparrow}$ and $\Sigma_{1\downarrow}$ Gaussians and the poor fit at the Fermi edge result from an inadequate representation of the background by a single Gaussian function.

The corresponding AREDC taken at 710 °C exhibits fewer features. Emission from the lower $\Sigma_{1\downarrow}$ band and the $\Sigma_{1\uparrow}$ band is still visible but less pronounced. Even without computer modeling, it is fairly clear that the $\Sigma_{1\uparrow}$ peak binding energy decreases. Also, the predominant peak composed of $\Sigma_{4\uparrow}$, $\Sigma_{1\downarrow}$, and $\Sigma_{3\downarrow}$ shifts down suggesting that the

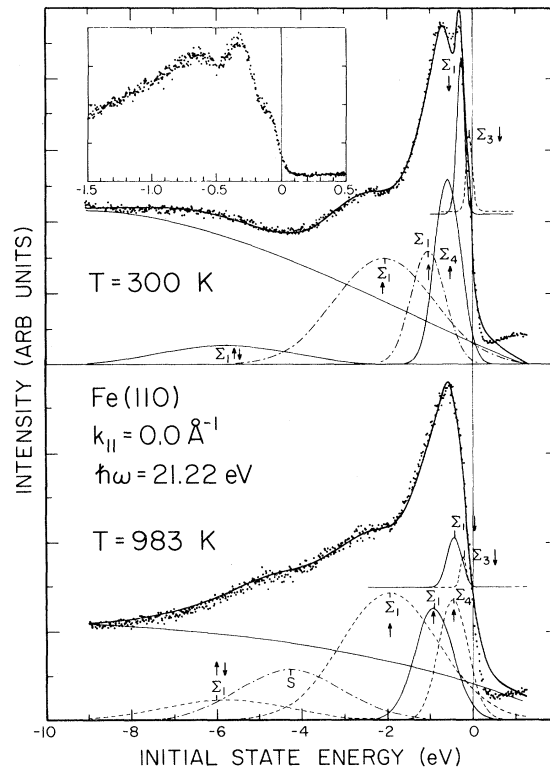


FIG. 3. Normal emission AREDC's for a Fe(110) surface at room temperature (upper figure) and at 710 °C (lower figure). Inset shows extended energy scale around E_F . Dots represent data, lines through the dots show the Gaussian fit. The six (upper figure) and seven (lower figure) Gaussians represent all components of the Gaussian model fit.

binding energies of minority spin bands decrease. This is consistent with the Stoner model of itinerant ferromagnetism. The Gaussian decomposition suggests the shift between $\Sigma_{1\uparrow}$ and $\Sigma_{1\downarrow}$ is about 200 meV for this temperature variation. This value is reasonable based on what Eastman *et al.*¹² observed for the temperature dependent component of exchange splitting at P .

Gaussian modeling of the peaks yields values for their strengths and widths in addition to their center positions. The full width at half maximum (FWHM) of peaks which are characterized well enough experimentally to yield reliable curve fits is found to increase with initial state energy. The initial state lifetime characterized by this width depends on Auger recombination which typically leaves two hole states just below E_F and an electron in a state just above E_F . Phase space arguments based on the filled and empty states available to participate in this process yield a linear line width behavior for Ni which has a high density of filled and unfilled states near E_F .²⁰ The same argument applies to iron except the band

width is slightly broader.

In summary, we have obtained the room-temperature exchange splitting at Γ and several critical point binding energies for electronic states of ferromagnetic iron. All of the peaks in our AREDC's can be accounted for in terms of theoretical calculations by assuming they result from direct interband transitions to a free electron final band. Difficulty was encountered in assigning some of the closely spaced peaks and some surface sensitivity was observed in several AREDC structures indicating possible contributions from surface states. The temperature dependence of the exchange splitting near Σ was

observed to be consistent with similar results near P reported recently. Many of the difficulties encountered in peak assignment can clearly be overcome by utilizing polarization selection rules and a continuously tunable photon source. This will require experimental work using synchrotron radiation.

ACKNOWLEDGMENT

This work was supported by the National Science Foundation under Grant No. DMR-79-23629.

-
- ¹D. G. Dempsey and L. Kleinman, Phys. Rev. Lett. **39**, 1297 (1977).
²L. Kleinman, Phys. Rev. B **22**, 6468 (1980).
³L. Kleinman, W. R. Grise, and K. Mednick, Phys. Rev. B **22**, 1105 (1980).
⁴J. Callaway and C. S. Wang, Phys. Rev. B **16**, 2095 (1977).
⁵D. J. Dempsey, L. Kleinman, and E. Caruthers, Phys. Rev. B **12**, 2932 (1975); **13**, 1489 (1976); **14**, 279 (1976); **14**, 288 (1976).
⁶M. Tomasek and P. Mikusik, Phys. Rev. B **8**, 410 (1973).
⁷M. C. Desjonqueres and F. Cyrot-Lackman, J. Phys. F **5**, 1368 (1975).
⁸C. S. Wang and A. J. Freeman, Phys. Rev. B (in press).
⁹P. Heiman and H. Neddermeyer, Phys. Rev. B **18**, 3537 (1978).
¹⁰A. Schultz, R. Courths, H. Schultz, and S. Hufner, J. Phys. F **9**, L41 (1979).
¹¹D. Kevan, P. S. Wehner, and D. A. Shirley, Solid State Commun. **28**, 517 (1978).
¹²D. E. Eastman, F. J. Himpsel, and J. A. Knapp, Phys. Rev. Lett. **44**, 95 (1980).
¹³J. L. Erskine, Phys. Rev. Lett. **45**, 1446 (1980).
¹⁴Interpretation of angle-resolved photoemission data based on direct transition model has been described in several papers. Comprehensive discussions are given by: T. C. Chiang, J. A. Knapp, M. Aono, and D. E. Eastman, Phys. Rev. B **21**, 3513 (1980), and by W. Eberhardt and E. W. Plummer [Phys. Rev. B **21**, 3245 (1980)].
¹⁵Cooper provides a good example: E. Dietz and D. E. Eastman, Phys. Rev. Lett. **41**, 1674 (1978).
¹⁶J. Hermanson, Solid State Commun. **22**, 9 (1977).
¹⁷W. Eberhardt and F. J. Himpsel, Phys. Rev. B **21**, 5572 (1980).
¹⁸We chose Σ because He I is the strongest line available, and we wanted to minimize effects due to sulphur diffusion which occurred during heating of the sample.
¹⁹Lorentzian line shapes are more appropriate, see, for example, D. E. Eastman, J. A. Knapp, and F. J. Himpsel, Phys. Rev. Lett. **41**, 825 (1978). The Gaussian fits are excellent and are clearly adequate to determine peak parameters.
²⁰Eberhardt and Plummer, Ref. 14.